AGU ADVANCING EARTH AND SPACE SCIENCES

Geophysical Research Letters

RESEARCH LETTER
10.1029/2024GL110962

Future Anthropogenic Land Use Change Impacts on Carbonaceous Aerosol and Implications for Climate and Air Quality

Yang Shi[1], **Colette L. Heald**[1,2], **and Maria Val Martin**[3]

[1]Civil and Environmental Engineering Department, Massachusetts Institute of Technology, Cambridge, MA, USA, [2]Institute for Atmospheric and Climate Science, ETH Zurich, Zurich, Switzerland, [3]School of Biosciences, University of Sheffield, Sheffield, UK

Key Points:

- Future anthropogenic land use change (LUC) will perturb biogenic and fire emissions, thereby modulating atmospheric carbonaceous aerosol
- The predicted change in carbonaceous aerosol loading results in moderate future aerosol direct radiative forcing
- Anthropogenic LUC may be more important than anthropogenic emissions in determining future carbonaceous aerosol burden

Supporting Information:

Supporting Information may be found in the online version of this article.

Correspondence to:

Y. Shi and C. L. Heald,
yangshi@mit.edu;
colette.heald@env.ethz.ch

Citation:

Shi, Y., Heald, C. L., & Val Martin, M. (2025). Future anthropogenic land use change impacts on carbonaceous aerosol and implications for climate and air quality. *Geophysical Research Letters*, *52*, e2024GL110962. https://doi.org/10.1029/2024GL110962

Received 21 JUN 2024
Accepted 21 FEB 2025

Abstract Future anthropogenic land use change (LUC) may alter atmospheric carbonaceous aerosol (black carbon and organic aerosol) burden by perturbing biogenic and fire emissions. However, there has been little investigation of this effect. We examine the global evolution of future carbonaceous aerosol under the Shared Socioeconomic Pathways projected reforestation and deforestation scenarios using the CESM2 model from present-day to 2100. Compared to present-day, the change in future biogenic volatile organic compounds emission follows changes in forest coverage, while fire emissions decrease in both projections, driven by trends in deforestation fires. The associated carbonaceous aerosol burden change produces moderate aerosol direct radiative forcing (−0.021 to +0.034 W/m^2) and modest mean reduction in $PM_{2.5}$ exposure (−0.11 μg/m^3 to −0.23 μg/m^3) in both scenarios. We find that future anthropogenic LUC may be more important in determining atmospheric carbonaceous aerosol burden than direct anthropogenic emissions, highlighting the importance of further constraining the impact of LUC.

Plain Language Summary Land is an important source for carbon-containing aerosols—fires emit soot and organics, while forests emit organic gases that form organic aerosols through chemical reactions in the atmosphere. Future anthropogenic activities, including reforestation and cropland expansion, may change the land use type and thus perturb the carbon-containing aerosols in the atmosphere. However, there has been little investigation on this topic. In this work, we study how the carbon-containing aerosol may change from the present to the end of the century under projected reforestation and deforestation pathways using a global climate model. We find that biogenic emissions follow the forest coverage, and fire emissions decrease in both projections due to a reduction in tropical anthropogenic deforestation by the end of the century. The resulting change in carbon-containing aerosol moderately cool or warm the climate at the end of the century because aerosols can scatter and/or absorb solar radiation. It also leads to a modest improvement in global air quality. We highlight the importance of further constraining the impact of future anthropogenic land use change, since we find that it may be even larger than the impact of anthropogenic emissions on the loading of carbon-containing aerosols in the atmosphere.

1. Introduction

Carbonaceous aerosols, including organics (both primary, POA and secondary, SOA) and black carbon (BC), make up 20%–80% of the fine aerosol mass in the troposphere (Jimenez et al., 2009; Zhang et al., 2007). These particles alter the Earth's climate directly through scattering and absorbing radiation and indirectly through perturbing cloud properties (Chung & Seinfeld, 2002). They also contribute to surface fine particulate matter ($PM_{2.5}$, i.e., particulate matter with diameter smaller than 2.5 μm), exposure to which is harmful for human health (Burnett et al., 2018). It is therefore crucial to estimate how carbonaceous aerosol levels will evolve in a future atmosphere.

Human activities have substantially altered global landscapes, converting 37% of land area into cropland and grazing land (Klein Goldewijk et al., 2017). The terrestrial biosphere is an important source of trace gases and aerosols, and thus anthropogenic land use change (LUC), such as forestry management and agricultural development, may critically impact atmospheric composition (Heald & Spracklen, 2015; Ward & Mahowald, 2015; Ward et al., 2014). This represents an underexplored anthropogenic forcing on climate.

Changes to vegetation and fire activity associated with LUC can modulate the sources of carbonaceous aerosol and its precursors. Natural vegetation produces biogenic volatile organic compounds (BVOCs), which oxidize in the atmosphere to form lower volatility products which can condense to form SOA (Hallquist et al., 2009). The emissions of BVOCs strongly depend on the vegetation type. For example, broadleaf trees are stronger emitters than crops and grasses (Guenther et al., 2012). Therefore, deforestation (reforestation) has been found to be associated with decrease (increase) in biogenic SOA concentrations (Heald & Geddes, 2016; Heald et al., 2008; Unger, 2014; Weber et al., 2024). Wildfires emit BC, POA, and SOA precursors. LUC influences fire emissions by altering the above-ground biomass and thus fuel availability (Kloster et al., 2010, 2012) and through socio-economic changes linked to conversion between natural and anthropogenic landscapes, such as savannah to cropland (Andela et al., 2017). In addition, deforestation fires in the tropics are a critical and variable source of emissions (Li et al., 2018; van der Werf et al., 2010), contributing ∼20% of global carbon emissions in present day (PD) (Li et al., 2013; van der Werf et al., 2010, 2017).

Anthropogenic LUC is projected to continue to the end of this century. Recent predictions from the Shared Socioeconomic Pathways (SSPs) suggest that total cropland may expand or contract in the future, accompanied by changes in forests and other natural lands (Riahi et al., 2017). However, there has been little exploration of how future LUC itself will impact carbonaceous aerosols and the attendant climate forcing and air quality. Previous studies suggested that anthropogenic LUC will alter the SOA burden by −20%–30% by 2100 from PD (Heald et al., 2008; Lund et al., 2021; Scott et al., 2018; Ward et al., 2014; Wu et al., 2012). But these studies either used LUC from old scenarios that only consider deforestation or applied idealized land use perturbations. Kloster et al. (2012) tested different Representative Concentration Pathway (RCP) scenarios and estimated that projected LUC and wood harvest would decrease total fire carbon emissions by 5%–35%, but they did not extend their results to atmospheric aerosols. Ward et al. (2014) found that LUC could modify fire aerosol emissions by −21%–21% from 2010 to 2100, depending on RCP trajectories. However, the radiative forcings associated with these LUC-driven fire aerosol changes were not estimated.

2. Methods

2.1. CLM5 and CAM6-Chem

We use the land and atmosphere components of the Community Earth System Model version 2.2 (CESM2.2; Danabasoglu et al., 2020)—Community Land Model version 5 (CLM5; Lawrence et al., 2019) and Community Atmosphere Model version 6 with chemistry (CAM6-Chem; Emmons et al., 2020).

The active biogeochemistry configuration of the CLM5 model used here prognostically calculates leaf area index (LAI). It includes 16 natural plant functional types and 8 active crops, which we grouped into seven land use types (i.e., tropical, temperate, and boreal tree, grass, shrub, crop, and bare soil) in the analysis for simplicity. BVOC emissions respond to light, temperature, leaf age, and CO_2 following the Model of Emissions of Gases and Aerosols from Nature (MEGAN) version 2.1 (Guenther et al., 2012). A prognostic fire model predicts smoke emissions (Li & Lawrence, 2017; Li et al., 2012, 2013), accounting for four types of fires: agricultural fires in cropland, deforestation fires in tropical closed forest, non-peat fires outside cropland and tropical closed forest, and peat fires. Fire burned area is determined by climate factors, vegetation properties, and human activities. The deforestation fire burned area is also related to the annual loss of tropical tree cover at each grid cell. Fire carbon emissions are estimated considering burned area and surface carbon density; emissions of trace gases and aerosol species are scaled from the fire carbon emissions using emission factors, which are dependent on the vegetation type. Peat fire emissions are unaffected by LUC and thus excluded from our analyses below (Figure S1 in Supporting Information S1). This fire model has been extensively evaluated and widely used by previous studies (see Texts S1.1 and S1.2 in Supporting Information S1), but we note that further work is needed to evaluate how well the model responds to LUC perturbations. Species emitted from biogenic and fire sources are tabulated in Table S1 in Supporting Information S1.

The CAM6-Chem model includes the MOZART-TS1 chemistry (Model of Ozone and Related chemical Tracers with tropospheric and stratospheric chemistry; Emmons et al., 2020) and a 4-mode version of the modal aerosol model (MAM4; Text S2 in Supporting Information S1 and Liu et al., 2016). Three carbonaceous aerosols (i.e., BC, POA, and SOA) are represented in MAM4. BC and POA are emitted from both fire and anthropogenic sources. All the fire emissions are injected into the model surface layer without considering the plume injection height (Val Martin et al., 2010), which is highly uncertain; previous studies disagree on the importance of this

factor (Carter et al., 2020; Lu et al., 2024; Tang et al., 2022; Veira et al., 2015). SOA formation from the oxidation of VOCs is parameterized through the volatility basis set that considers NO_x-dependent yields (Hodzic et al., 2016; Jo et al., 2021; Tilmes et al., 2019). VOCs precursors for SOA formation are also shown in Table S1 in Supporting Information S1.

2.2. Experiments

We conducted model experiments in two steps: (a) estimating biogenic and fire emissions with evolving anthropogenic LUC using CLM5 and then (b) exploring the climate and the air quality impacts of the LUC-driven carbonaceous aerosol changes using CAM6-Chem.

For the first step, two CLM5 experiments were conducted using land use data following the SSP1-2.6 and SSP3-7.0 pathways (hereafter SSP1 and SSP3; Riahi et al., 2017). These two pathways are chosen because they bracket the range of projected global reforestation (SSP1) and deforestation (SSP3). But we note that in SSP1 (SSP3) there may be local deforestation (reforestation) (Figure S2 in Supporting Information S1). Initially, we spun up CLM5 to steady state in 1850 for about 1,200 years to reach equilibrium. Subsequently, a spin-up from 1850 to 2004 was conducted using historical data. The two future simulations were run from 2005 to 2100, with meteorology cycling from 2001 to 2010 following offline data set, CO_2 concentrations fixed to year 2005, and population density fixed to year 2010. Simulated biogenic and fire emissions were averaged over the first (2005–2014) and last (2091–2100) 10 years of the simulations to generate climatologically monthly emission files for PD and future (F) conditions. We note that both SSP1 and SSP3 simulations have the same PD emissions because the land use data are identical before 2015. The annual total fire carbon emission for PD (2720 Tg/yr) falls within the range of Global Fire Emission Database version 4.1s (GFED4.1s; 2027 Tg/yr; Randerson et al., 2018) and Fire Inventory from NCAR version 2.5 (FINNv2.5; 3399 Tg/yr; Wiedinmyer et al., 2023a, 2023b) over the same years with few regional exceptions (Table S2 in Supporting Information S1; see Figure S3 and Text S1.3 in Supporting Information S1 for comparisons in spatial patterns), which indicates a reasonable representation of the fire emission in the CLM5 fire model.

For the second step, we performed three CAM6-Chem experiments (one PD and two F) driven by the biogenic and fire emissions generated from the CLM5 experiments. Anthropogenic emissions were set to PD climatology (Hoesly et al., 2018) in all the three experiments. By comparing the two F experiments with the PD experiment, we estimate the climate and air quality impacts of LUC-driven carbonaceous aerosol change. In addition, to investigate the relative importance of LUC and anthropogenic emissions, another two CAM6-Chem experiments were conducted using future SSP1-2.6 and SSP3-7.0 anthropogenic emissions (Riahi et al., 2017) but keeping biogenic and fire emissions and climate at PD (see Section 3.4). Anthropogenic emissions related to carbonaceous aerosols include those for BC, POA, and anthropogenic VOCs (Table S1 in Supporting Information S1). All simulations were performed for 11 years with the first year used for spin-up at $0.9° \times 1.25°$ horizontal resolution and 32 vertical layers.

In each CAM6-Chem experiment, we added diagnostic radiative calls that remove total carbonaceous aerosol and each carbonaceous aerosol species, respectively, to estimate the effective radiative forcing due to aerosol-radiation interaction (ERF_{ari}; also known as direct radiative forcing) from PD to F. We first calculated the direct radiative effects by taking the difference between default radiative fluxes and those from diagnostic calls that remove corresponding aerosol species. Then, the ERF_{ari} was defined as the direct radiative effect in F with respect to PD. We note that we do not account for the radiative forcing related to aerosol-cloud interactions (i.e., indirect forcing).

3. Result

3.1. Emissions Response to LUC

We first explore the LUC from PD to F as well as the corresponding changes in BVOC and fire emissions using the CLM5 simulations (Figures 1a–1c). The SSP1 scenario projects reforestation over tropical and temperate forest accompanied by cropland expansion at the expense of grassland (Figure 1a). Tropical reforestation is predominantly concentrated in Eastern Brazil and tropical Africa except the Congo Basin, while temperate tree reforestation occurs in the Eastern US, Europe, and Eastern China (Figures S2a and S2b in Supporting Information S1). In contrast, SSP3 forecasts a deforestation of tropical trees, primarily in tropical Africa and the

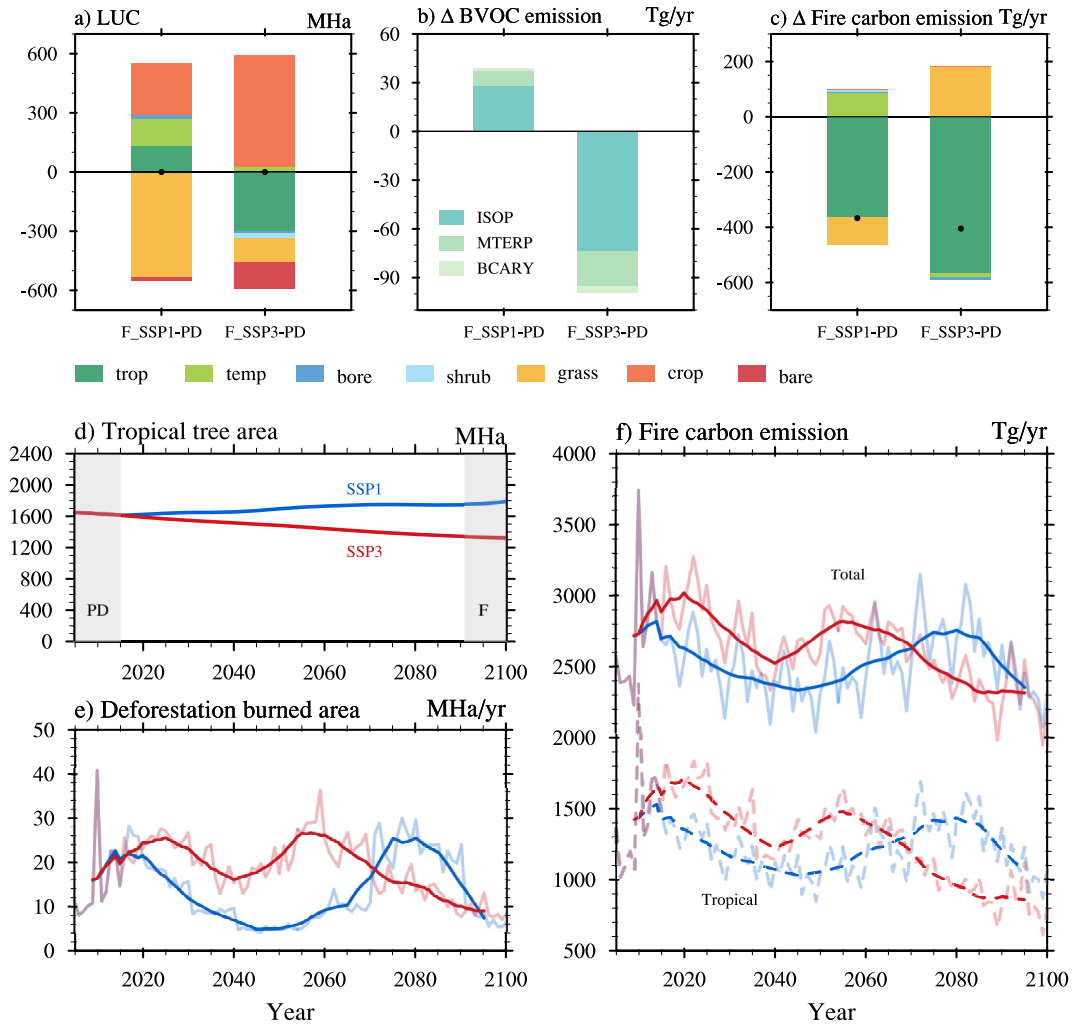

Figure 1. (a) LUC (b) BVOC (ISOP: isoprene, MTERP: monoterpene, and BCARY: sesquiterpene) emission change, and (c) total fire carbon emission change from PD to F projected by SSP1 and SSP3. LUC and fire carbon emission change are shown in land use classes (trop: tropical tree, temp: temperate tree, bore: boreal tree, shrub, grass, crop, and bare: bare soil) and categorized by colors. Black dots on panel (a, c) are global total changes. Panels (d–f) show SSP1 (blue lines) and SSP3 (red lines) projections of tropical tree area, deforestation burned area, and fire carbon emission, respectively. Gray shading on panel (d) marks the time periods treated as PD (2005–2014) and F (2091–2100). Light red and blue lines on panel (e, f) are yearly time series, while darker lines are 10 year running means. On panel (f), solid and dashed lines are total fire carbon emission and that from tropical tree, respectively. Figure S4 in Supporting Information S1 reproduces this figure in a color-blind friendly version.

western Amazon Forest (Figure S2h in Supporting Information S1), along with a moderate global reduction in grassland and bare soil and a substantial increase in cropland (Figure 1a). We observe that, in SSP3, the change in grassland area is not globally uniform—in particular, the African grassland change exhibits a dipole feature, characterized by a significant increase in the Congo Rainforest and the Sahel but a decrease elsewhere (Figure S2l in Supporting Information S1).

The global total emissions for BVOCs, BC, and POA in PD and F are shown in Table S3 in Supporting Information S1. In response to the reforestation in SSP1 and the deforestation in SSP3, total BVOC emissions, including isoprene, monoterpenes, and sesquiterpenes, increase by 39 Tg/yr (5.6%) and decreases by 99.3 Tg/yr (14.2%) in SSP1 and SSP3, respectively (Figure 1b). The percentage change is consistent among the three classes of biogenic VOCs. The spatial distribution of the change in BVOC emissions is generally positively correlated with the alteration of tree coverage (Figures S2 and S5 in Supporting Information S1). In the SSP1 scenario, emissions increase in Eastern US, Southern Africa, Europe, and Eastern China. The Amazon forest also shows

slight BVOC emissions increase (mostly <2%) but has little LUC, which is related to LAI increases (Figure S6 in Supporting Information S1). In the SSP3 scenario, the emissions decrease in the Southern Hemisphere (SH; South America and Africa), India, Southeast Asia, and the East Coast of the US, whereas emissions increase in the Midwest and South US, Europe, and Eastern China.

The total fire carbon emissions decrease by 367 Tg/yr in SSP1 and by 404.8 Tg/yr in SSP3 (Figure 1c). This converts to a BC emission decrease of 0.4 TgC/yr (3.7%) in both F projections and a POA emission decrease of 3.4 TgC/yr (5.6%) and 5.5 TgC/yr (9.1%) in SSP1 and SSP3, respectively (Table S3 in Supporting Information S1). The fire carbon emissions decrease is dominated by tropical forest in both projections, despite the opposite changes in tropical forest extent (Figures 1c and 1d). The fire emissions decrease in SSP1 (reforestation scenario) reflects the decrease in tropical deforestation fires, outweighing the growth in fuel availability caused by tropical reforestation (Figures 1e and 1f). Although global tropical tree coverage increases persistently in SSP1, regional tropical tree loss exists, peaking around 2080 (Figure S7 in Supporting Information S1). In SSP3 (deforestation scenario), the tropical tree loss and associated deforestation fires is stronger in the first half of the century, peaking around 2020 and 2055. In the latter half of the century, deforestation fires decline and the overall reduction in forest biomass over the tropics generate less fire carbon loss. Thus, the total F (2091–2100) fire emissions are less than in PD. Our results indicate that around half of the emissions originate from tropical forests (Figure 1f). This may be an overprediction, because GFED4.1s suggests that tropical savannas account for 62% of total fire carbon emissions (van der Werf et al., 2017). But it is worthwhile to note that satellite-based fire emission products also rely on uncertain factors, like biogeochemical models, land cover data sets, and emission factors. In addition, in the SSP3 projection, the global fire carbon emission from grassland increases despite the global grassland coverage decreases (Figures 1a and 1c). This reflects the heterogeneous response of fire carbon emission to LUC over grassland, which is related to vegetation density (Figure S8 in Supporting Information S1).

The fire emissions projected with the SSP1 LUC scenario show declines in the tropics but growth in subtropics and the mid-latitudes (Figure S9 in Supporting Information S1). In SSP3, the fire emissions are projected to mostly decrease in the tropics and the SH (Figure S9 in Supporting Information S1), in response to the tropical deforestation and grassland shrink. However, there is an emission increase in the Congo Basin, which is the combined result of both deforestation fire and grassland coverage increase. The conversion from grassland into cropland decreases local fire emissions over South Africa and India in SSP3 (Text S1.4 in Supporting Information S1). We note that the LUC in the Eastern US, Europe, and Eastern and Southern China are relatively strong in both predictions but the changes in fire emission are minor, which reflects the suppression of fire in these highly populated regions (Text S1.5 in Supporting Information S1). Also, both scenarios show emission perturbations in East Siberia (in total, less than 2 Tg/yr) that may be related to disturbance in soil moisture and other factors rather than LUC.

3.2. Carbonaceous Aerosol Burden Change and Climate Forcing

In the SSP1, the global carbonaceous aerosol burden increases marginally by 0.003 Tg (0.15%) (Figure 2a), which results from an increase in SOA (0.038 Tg; 4.4%), driven by biogenic emission increases, mostly compensated by decreases in the fire-driven BC (−0.005 Tg; −3.9%) and POA (−0.03 Tg; −3.9%) (Figure 2c). In the SSP3, the burden of all the three aerosol species decreases (SOA: −0.175 Tg, −20.2%; BC: −0.006 Tg, −4.7%; POA: −0.079 Tg, −10.2%), following the decreases in both biogenic and fire emissions (Figure 2c). This leads to a substantial total carbonaceous aerosol burden decrease (−0.26 Tg, −12.6%) (Figure 2b). The two scenarios result in particularly different trajectories over the SH (Figures 2a and 2b)—the carbonaceous aerosol burden decreases significantly and consistently in the SH in SSP3, whereas in SSP1, the change is largely positive. Given the relatively short lifetime of aerosols, the spatial distribution of the burden change generally follows local emission changes (Figures S10a–S10f in Supporting Information S1). We notice that the aerosol lifetime changes slightly from PD to F due to changing geographical distribution of emissions (Table S4 in Supporting Information S1).

Carbonaceous aerosols impact the climate through direct interactions with shortwave radiation—POA and SOA have net cooling radiative effect through scattering shortwave radiation, while BC is a light-absorbing aerosol that has a strong warming effect. We note here that given uncertainties in the sources and photochemical evolution of brown carbon, we neglect the warming effect of this contribution to POA and SOA. This may be somewhat compensated by fire aerosols that are too strongly absorbing (Brown et al., 2021). For SSP1, the global averaged ERF_{ari} due to LUC-driven total carbonaceous aerosol change is −0.021 W/m^2 (Figure 2d), which is dominated by

10.1029/2024GL110962

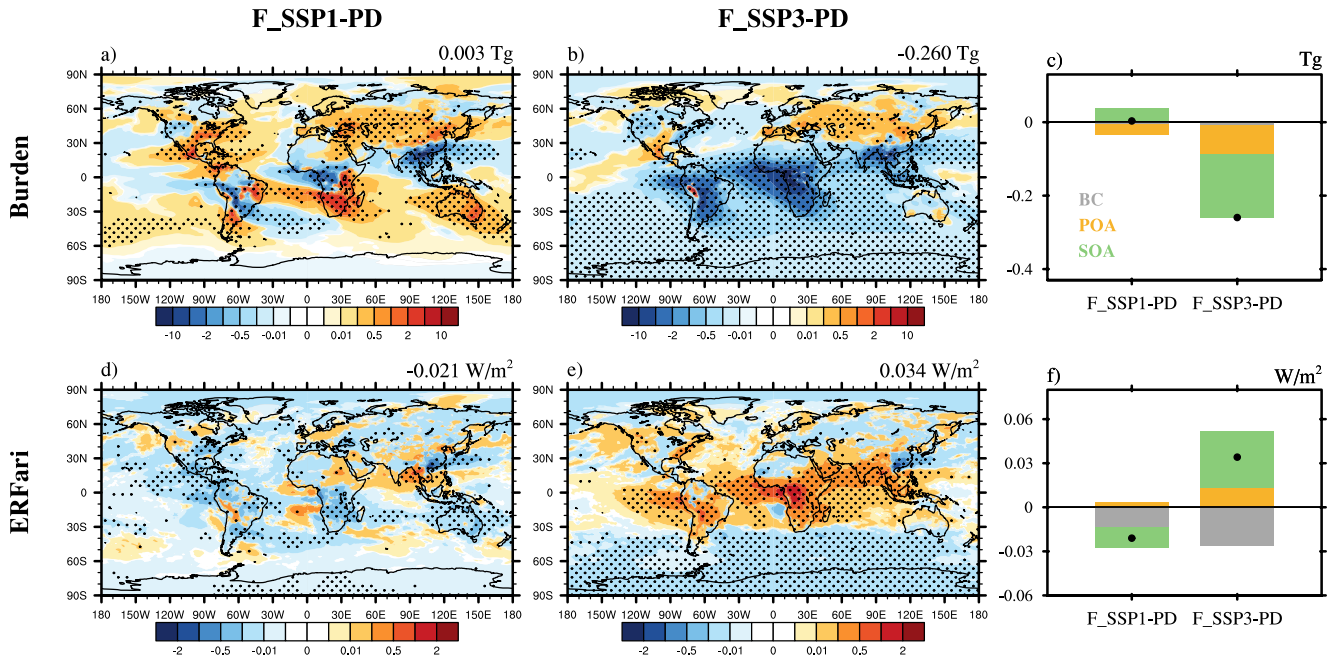

Figure 2. Annual change in total carbonaceous aerosol burden (top row; unit: mg/m^2) and the ERF$_{ari}$ from PD to future (bottom row; unit: W/m^2). Dotted regions on panel (a, b, d, e) are where the changes are significant to the 0.05 levels. Numbers on the top right of each panel are global total burden (a, b) and global average ERF$_{ari}$ (d, e). Also shown are global total burden (c) and global averaged ERF$_{ari}$ (f) with contribution from individual aerosol species classified by colors. Black dots on the two panels (c, f) are changes in total carbonaceous aerosols.

a cooling due to the BC burden decrease and the SOA burden increase that overweighs the warming caused by the POA burden decrease (Figure 2f). In SSP3, the decrease in POA and SOA burden results in a strong warming ERF$_{ari}$ whereas there is a moderate cooling caused by BC burden decrease. As a result, the global ERF$_{ari}$ for total carbonaceous aerosol is +0.034 W/m^2 in SSP3 (Figure 2e). The warming predominantly occurs over the tropical and subtropical regions in the SH, with regional forcing that exceeds 0.1 W/m^2. We note that the decreasing aerosol burden at mid and high southern latitudes leads to a cooling due to preponderance of POA and SOA above cloud during the poleward transport in the SH. Overall, the future LUC-driven ERF$_{ari}$ of the carbonaceous aerosol in both projections are on the order of ∼10% of the total aerosol ERF$_{ari}$ (−0.3 ± 0.3 W/m^2) from 1750 to 2014 estimated by IPCC AR6 (Forster et al., 2021).

We find that SOA has the largest burden change among the three aerosol species in both future predictions. Moreover, the ERF$_{ari}$ from the fire aerosols (i.e., BC and POA) oppose each other and produce a forcing that is smaller in magnitude compared to that of SOA. Therefore, we conclude that the LUC-driven biogenic emissions have larger impact on carbonaceous aerosol burden and climate forcing than the LUC-driven fire emissions in these simulations.

3.3. Surface PM$_{2.5}$

LUC-driven changes in carbonaceous aerosol, which contribute to surface PM$_{2.5}$, have implications for human health. Figures 3a and 3b shows the global distributions of surface carbonaceous aerosol PM$_{2.5}$ concentration change from PD to F. In contrast to the burden increase, global averaged surface PM$_{2.5}$ concentrations decrease by −0.031 μg/m^3 (−5.1%) in the SSP1 projection. This difference is due to the change in SOA, whose global burden increases (Figure S10c in Supporting Information S1) but surface concentration slightly decreases (Figure S11c in Supporting Information S1). The strongest decrease occurs over the tropics, including the Amazon Forest, mid-Africa, and Southeast Asia. These regions have dense forest and therefore large BVOC emissions (Guenther et al., 2012). As a result, surface OH is depleted and the SOA formation timescale is extended, making surface SOA levels rather insensitive to VOC emission increases. Instead, the fire-driven decrease in POA concentration has a larger impact on SOA by limiting the condensation of precursor gases. Therefore, the change in surface SOA concentration mostly follows the POA change in the tropics (Figures S11b and S11c in Supporting

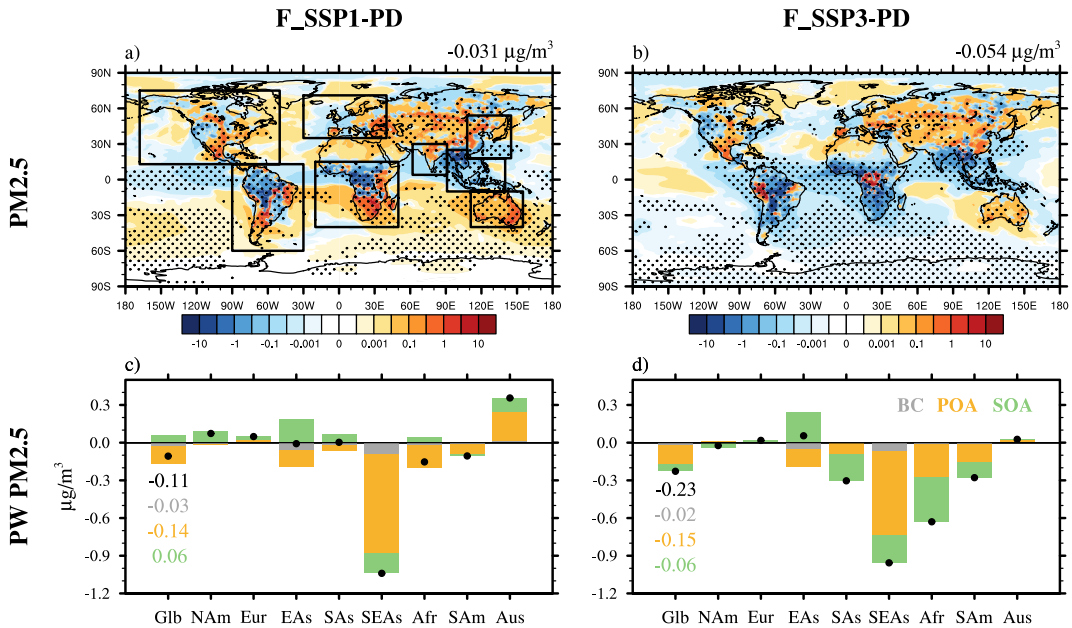

Figure 3. Top row: same as panel (a, b) in Figure 2, except for total carbonaceous aerosol $PM_{2.5}$ surface concentrations. Global (Glb) and regional (NAm: North America, Eur: Europe, EAs: East Asia, SAs: South Asia, SEAs: Southeast Asia, Afr: Africa, SAm: South America, Aus: Australia) average surface population weighted (PW) $PM_{2.5}$ concentrations are shown on the bottom panels (c, d). Borders of regions are shown by black rectangles in panel (a). On panels (c, d), contributions from individual species are classified by different colors, while the black dots represent total changes. Global averaged total PW $PM_{2.5}$ concentrations are given in black numbers, with contribution from each aerosol species shown by numbers in corresponding colors.

Information S1). In the SSP3 projection, the surface total $PM_{2.5}$ concentration decreases by −0.054 μg/m^3 (−8.9%), because of reductions in all three aerosol species. The change in surface SOA is due to changes in both BVOC emissions and surface POA concentrations.

To estimate the impact of the change in carbonaceous aerosols on human $PM_{2.5}$ exposure, we calculate the global and regional population weighted (PW) $PM_{2.5}$ changes (Figures 3c and 3d). We use 2010 from the Gridded Population of the World, Version 4 data set (SEDAC, 2018) for both PD and F. Globally, the total surface PW $PM_{2.5}$ concentration decreases in both SSP1 (by −0.11 μg/m^3) and SSP3 (by −0.23 μg/m^3). The reduction in both projections is dominated by the change in POA concentrations driven by decreases in fire emission. The global averaged improvement in air quality in both projections is modest comparing to the World Health Organization air quality guideline level (5 μg/m^3; WHO, 2021), with larger regional improvements (e.g., nearly 1 μg/m^3 over Southeast Asia).

Globally, the fire aerosols drive the reductions in PW $PM_{2.5}$ surface concentrations, both directly and via changing the partitioning of SOA. Therefore, from our simulations we conclude that the air quality response to anthropogenic LUC is dominated by the trajectory of fire emissions. We note that our conclusions here and in Section 3.2 are both subjected to uncertainties related to fire plume injection heights—injecting smoke emissions aloft will reduce the LUC-driven fire PW $PM_{2.5}$ decrease at the surface and may impact aerosol transport and climate radiative effects (See Figure S12 and Text S3 in Supporting Information S1).

3.4. Relative Importance of LUC and Anthropogenic Emissions Changes

Anthropogenic emissions of carbonaceous aerosol are projected to change in the next century in response to socio-economic factors, including air quality regulation. The SSP1 is a strong pollution control scenario, which exhibits a rapid decline globally in anthropogenic emissions (Figure 4c; Figures S13 and S14 in Supporting Information S1). In contrast, the SSP3 scenario assumes that the implementation of pollution controls is delayed. Therefore, anthropogenic emissions increase slightly over the short-term, except over developed regions, and declines in the second half of the century when strong emission reductions also occur in Asia (Figure S13 in

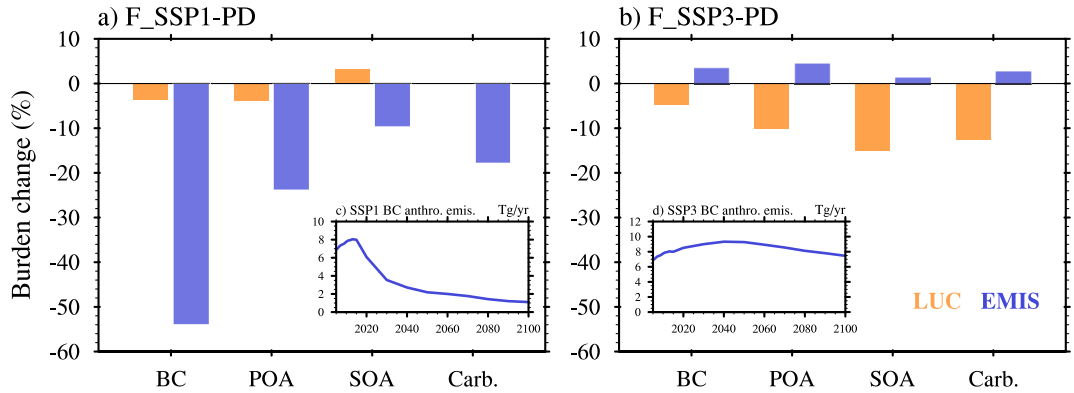

Figure 4. Percentage change in atmospheric carbonaceous aerosol burden in the two future scenarios compared with PD, for (a) F_SSP1 and (b) F_SSP3. Bars represent the impact of anthropogenic LUC (orange) and anthropogenic emission (EMIS, blue) changes. Inset panels are time series for anthropogenic BC emissions following (c) SSP1 and (d) SSP3.

Supporting Information S1). As a result, the end of century emissions in SSP3 are comparable to the level at PD (Figure 4d; Figure S14 in Supporting Information S1).

Figure 4 compares the percentage change in atmospheric carbonaceous aerosol burden due to anthropogenic LUC and anthropogenic emissions change. In the SSP1 projection, the reduction in anthropogenic emissions has a more substantial impact on carbonaceous aerosol burden than LUC. In contrast, the LUC-driven emission change plays a more important role in the SSP3 projection. Therefore, depending on which pathway we take, the impact of anthropogenic LUC may outweigh the impact of anthropogenic emission changes on the abundance of carbonaceous aerosol and, consequently, the climate forcing and air quality.

Previous studies suggest that climate change will increase future atmospheric carbonaceous aerosols (Heald et al., 2008; Kloster et al., 2012; Sporre et al., 2019). We conducted two additional CLM5 experiments and find that the magnitude of emission changes due to LUC is 25%–128% of that due to climate change (Figure S15 and Text S4 in Supporting Information S1), highlighting that both climate change and LUC have a substantial impact on carbonaceous aerosol sources.

4. Conclusions

In this study, we investigate the response of carbonaceous aerosols (i.e., BC, POA, and SOA) to future anthropogenic LUC using CESM2. We test two future LUC projections (SSP1-2.6 and SSP3-7.0), which bracket the range of reforestation and deforestation. In response to the forest coverage change, BVOC emissions increase in SSP1 and decrease in SSP3. However, fire emission decrease in both projections. Dynamically varying tropical fires dominate the fire emission trends. Therefore, the fire emissions do not monotonically follow LUC, which emphasizes that the time horizon selected to quantify the effect of LUC is critical. We find that the LUC-driven carbonaceous aerosol emission change by end of century results in a direct radiative forcing that is cooling in SSP1 and warming in SSP3, the magnitude of which are moderate as compared to the total historical ERF_{ari} for aerosol in IPCC AR6. Both future LUC scenarios result in modest improvements in air quality. Overall, with the two future pathways tested in this study, we conclude that the LUC-driven biogenic emissions may have a larger impact on climate forcing, while the LUC-driven fire emissions may be more important for air quality. We note that our study relies on existing land (including fire parameterizations and their relationship to land use change) and atmospheric models and commonly used SSP projections, all of which introduce uncertainties to our results. Given that we find that LUC represents a considerable perturbation to future carbonaceous aerosol concentrations, future research is needed to improve these model schemes and data sets to reduce the associated uncertainties.

Biogenic and fire aerosols are generally overlooked when quantifying aerosol climate forcing (e.g., in IPCC AR6 and the modeling studies it builds upon). Our work demonstrates that LUC is an anthropogenic mechanism that can alter these aerosols, regardless of whether their source is natural or anthropogenic. We find that this pathway may be an even more important driver than direct anthropogenic emissions in modifying atmospheric

carbonaceous aerosol burden and thus in determining the future climate forcing and air quality impact of carbonaceous aerosols. This highlights the importance of including these effects in future climate simulations and improving our understanding of how fire and biogenic emissions respond to changing land use as well as climate.

Data Availability Statement

Data sets used for model evaluation include the GFED4.1 fire emission data (Randerson et al., 2018), the FINNv2.5 fire emission data (Wiedinmyer et al., 2023b), and the global population data set (SEDAC, 2018). This work is based on CESM2.2 (NCAR, 2023). The data shown in the figures is available on Zenodo (Shi et al., 2025).

Acknowledgments
This work was supported by the U.S. National Science Foundation (AGS-2223070) and Department of Energy (DE-SC0022017). MVM is supported by the UKRI Future Leaders Fellowship Programme (MR/T019867/1). We gratefully acknowledge high-performance computing support from Cheyenne (https://doi.org/10.5065/D6RX99HX) provided by NCAR's Computational and Information Systems Laboratory, sponsored by the National Science Foundation.

References

Andela, N., Morton, D. C., Giglio, L., Chen, Y., van der Werf, G. R., Kasibhatla, P. S., et al. (2017). A human-driven decline in global burned area. *Science*, *356*(6345), 1356–1362. https://doi.org/10.1126/science.aal4108

Brown, H., Liu, X., Pokhrel, R., Murphy, S., Lu, Z., Saleh, R., et al. (2021). Biomass burning aerosols in most climate models are too absorbing. *Nature Communications*, *12*(1), 277. https://doi.org/10.1038/s41467-020-20482-9

Burnett, R., Chen, H., Szyszkowicz, M., Fann, N., Hubbell, B., Pope, C. A., et al. (2018). Global estimates of mortality associated with long-term exposure to outdoor fine particulate matter. *Proceedings of the National Academy of Sciences of the United States of America*, *115*(38), 9592–9597. https://doi.org/10.1073/pnas.1803222115

Carter, T. S., Heald, C. L., Jimenez, J. L., Campuzano-Jost, P., Kondo, Y., Moteki, N., et al. (2020). How emissions uncertainty influences the distribution and radiative impacts of smoke from fires in North America. *Atmospheric Chemistry and Physics*, *20*, 2073–2097. https://doi.org/10.5194/acp-20-2073-2020

Chung, S. H., & Seinfeld, J. H. (2002). Global distribution and climate forcing of carbonaceous aerosols. *Journal of Geophysical Research*, *107*(D19), 4407. https://doi.org/10.1029/2001JD001397

Danabasoglu, G., Lamarque, J.-F., Bacmeister, J., Bailey, D. A., DuVivier, A. K., Edwards, J., et al. (2020). The Community Earth System Model Version 2 (CESM2). *Journal of Advances in Modeling Earth Systems*, *12*(2), e2019MS001916. https://doi.org/10.1029/2019MS001916

Emmons, L. K., Schwantes, R. H., Orlando, J. J., Tyndall, G., Kinnison, D., Lamarque, J., et al. (2020). The Chemistry Mechanism in the Community Earth System Model Version 2 (CESM2). *Journal of Advances in Modeling Earth Systems*, *12*(4). https://doi.org/10.1029/2019MS001882

Forster, P., Storelvmo, T., Armour, K., Collins, W., Dufresne, J.-L., Frame, D., et al. (2021). The Earth's energy budget, climate feedbacks, and climate sensitivity. In V. P. Masson-Delmotte, et al. (Eds.), *Climate Change 2021: The Physical Science Basis. Contribution of Working Group I to the Sixth Assessment Report of the Intergovernmental Panel on Climate Change* (pp. 923–1054). Cambridge University Press. https://doi.org/10.1017/9781009157896

Guenther, A. B., Jiang, X., Heald, C. L., Sakulyanontvittaya, T., Duhl, T., Emmons, L. K., & Wang, X. (2012). The Model of Emissions of Gases and Aerosols from Nature version 2.1 (MEGAN2.1): An extended and updated framework for modeling biogenic emissions. *Geoscientific Model Development*, *5*(6), 1471–1492. https://doi.org/10.5194/gmd-5-1471-2012

Hallquist, M., Wenger, J. C., Baltensperger, U., Rudich, Y., Simpson, D., Claeys, M., et al. (2009). The formation, properties and impact of secondary organic aerosol: Current and emerging issues. *Atmospheric Chemistry and Physics*, *9*(14), 5155–5236. https://doi.org/10.5194/acp-9-5155-2009

Heald, C. L., & Geddes, J. A. (2016). The impact of historical land use change from 1850 to 2000 on secondary particulate matter and ozone. *Atmospheric Chemistry and Physics*, *16*(23), 14997–15010. https://doi.org/10.5194/acp-16-14997-2016

Heald, C. L., Henze, D. K., Horowitz, L. W., Feddema, J., Lamarque, J.-F., Guenther, A., et al. (2008). Predicted change in global secondary organic aerosol concentrations in response to future climate, emissions, and land use change: Future predicted change in global SOA. *Journal of Geophysical Research*, *113*(D5). https://doi.org/10.1029/2007JD009092

Heald, C. L., & Spracklen, D. V. (2015). Land use change impacts on air quality and climate. *Chemical Reviews*, *115*(10), 4476–4496. https://doi.org/10.1021/cr500446g

Hodzic, A., Kasibhatla, P. S., Jo, D. S., Cappa, C. D., Jimenez, J. L., Madronich, S., & Park, R. J. (2016). Rethinking the global secondary organic aerosol (SOA) budget: Stronger production, faster removal, shorter lifetime. *Atmospheric Chemistry and Physics*, *16*(12), 7917–7941. https://doi.org/10.5194/acp-16-7917-2016

Hoesly, R. M., Smith, S. J., Feng, L., Klimont, Z., Janssens-Maenhout, G., Pitkanen, T., et al. (2018). Historical (1750–2014) anthropogenic emissions of reactive gases and aerosols from the Community Emissions Data System (CEDS). *Geoscientific Model Development*, *11*(1), 369–408. https://doi.org/10.5194/gmd-11-369-2018

Jimenez, J. L., Canagaratna, M. R., Donahue, N. M., Prevot, A. S. H., Zhang, Q., Kroll, J. H., et al. (2009). Evolution of organic aerosols in the atmosphere. *Science*, *326*(5959), 1525–1529. https://doi.org/10.1126/science.1180353

Jo, D. S., Hodzic, A., Emmons, L. K., Tilmes, S., Schwantes, R. H., Mills, M. J., et al. (2021). Future changes in isoprene-epoxydiol-derived secondary organic aerosol (IEPOX SOA) under the Shared Socioeconomic Pathways: The importance of physicochemical dependency. *Atmospheric Chemistry and Physics*, *21*(5), 3395–3425. https://doi.org/10.5194/acp-21-3395-2021

Klein Goldewijk, K., Beusen, A., Doelman, J., & Stehfest, E. (2017). Anthropogenic land use estimates for the Holocene—HYDE 3.2. *Earth System Science Data*, *9*(2), 927–953. https://doi.org/10.5194/essd-9-927-2017

Kloster, S., Mahowald, N. M., Randerson, J. T., & Lawrence, P. J. (2012). The impacts of climate, land use, and demography on fires during the 21st century simulated by CLM-CN. *Biogeosciences*, *9*(1), 509–525. https://doi.org/10.5194/bg-9-509-2012

Kloster, S., Mahowald, N. M., Randerson, J. T., Thornton, P. E., Hoffman, F. M., Levis, S., et al. (2010). Fire dynamics during the 20th century simulated by the community land model. *Biogeosciences*, *7*(6), 1877–1902. https://doi.org/10.5194/bg-7-1877-2010

Lawrence, D. M., Fisher, R. A., Koven, C. D., Oleson, K. W., Swenson, S. C., Bonan, G., et al. (2019). The community land model version 5: Description of new features, benchmarking, and impact of forcing uncertainty. *Journal of Advances in Modeling Earth Systems*, *11*(12), 4245–4287. https://doi.org/10.1029/2018MS001583

Li, F., & Lawrence, D. M. (2017). Role of fire in the global land water budget during the twentieth century due to changing ecosystems. *Journal of Climate*, *30*(6), 1893–1908. https://doi.org/10.1175/JCLI-D-16-0460.1

Li, F., Lawrence, D. M., & Bond-Lamberty, B. (2018). Human impacts on 20th century fire dynamics and implications for global carbon and water trajectories. *Global and Planetary Change*, *162*, 18–27. https://doi.org/10.1016/j.gloplacha.2018.01.002

Li, F., Levis, S., & Ward, D. S. (2013). Quantifying the role of fire in the Earth system—Part 1: Improved global fire modeling in the Community Earth System Model (CESM1). *Biogeosciences*, *10*(4), 2293–2314. https://doi.org/10.5194/bg-10-2293-2013

Li, F., Zeng, X. D., & Levis, S. (2012). A process-based fire parameterization of intermediate complexity in a dynamic global vegetation model. *Biogeosciences*, *9*(7), 2761–2780. https://doi.org/10.5194/bg-9-2761-2012

Liu, X., Ma, P.-L., Wang, H., Tilmes, S., Singh, B., Easter, R. C., et al. (2016). Description and evaluation of a new four-mode version of the Modal Aerosol Module (MAM4) within version 5.3 of the community atmosphere model. *Geoscientific Model Development*, *9*(2), 505–522. https://doi.org/10.5194/gmd-9-505-2016

Lu, Z., Liu, X., Ke, Z., Zhang, K., Ma, P.-L., & Fan, J. (2024). Incorporating an interactive fire plume-rise model in the DOE's energy exascale earth system model version 1 (E3SMv1) and examining aerosol radiative effect. *Journal of Advances in Modeling Earth Systems*, *16*, e2023MS003818. https://doi.org/10.1029/2023MS003818

Lund, M. T., Rap, A., Myhre, G., Haslerud, A. S., & Samset, B. H. (2021). Land cover change in low-warming scenarios may enhance the climate role of secondary organic aerosols. *Environmental Research Letters*, *16*(10), 104031. https://doi.org/10.1088/1748-9326/ac269a

NCAR. (2023). Community Earth system model version 2.2.2 [Software]. *Github*. Retrieved from https://github.com/ESCOMP/CESM/releases/tag/cesm2.2.2

Randerson, J. T., van der Werf, G. R., Giglio, L., Collatz, G. J., & Kasibhatla, P. S. (2018). Global Fire Emissions Database, version 4.1 (GFEDv4) [Dataset]. *ORNL DAAC*. https://doi.org/10.3334/ORNLDAAC/1293

Riahi, K., van Vuuren, D. P., Kriegler, E., Edmonds, J., O'Neill, B. C., Fujimori, S., et al. (2017). The shared socioeconomic pathways and their energy, land use, and greenhouse gas emissions implications: An overview. *Global Environmental Change*, *42*, 153–168. https://doi.org/10.1016/j.gloenvcha.2016.05.009

Scott, C. E., Monks, S. A., Spracklen, D. V., Arnold, S. R., Forster, P. M., Rap, A., et al. (2018). Impact on short-lived climate forcers increases projected warming due to deforestation. *Nature Communications*, *9*(1), 157. https://doi.org/10.1038/s41467-017-02412-4

SEDAC. (2018). Gridded population of the world, version 4 (GPWv3): Population density, revision 11 [Dataset]. *NASA*. https://doi.org/10.7927/H49C6VHW

Shi, Y., Heald, C. L., & Val, M. (2025). Data from: Future anthropogenic land use change impacts on natural carbonaceous aerosol and implications for climate and air quality [Dataset]. *Zenodo*. https://doi.org/10.5281/zenodo.14873517

Sporre, M. K., Blichner, S. M., Karset, I. H. H., Makkonen, R., & Berntsen, T. K. (2019). BVOC-aerosol-climate feedbacks investigated using NorESM. *Atmospheric Chemistry and Physics*, *19*(7), 4763–4782. https://doi.org/10.5194/acp-19-4763-2019

Tang, W., Emmons, L. K., Buchholz, R. R., Wiedinmyer, C., Schwantes, R. H., He, C., et al. (2022). Effects of fire diurnal variation and plume rise on U.S. air quality during FIREX-AQ and WE-CAN based on the Multi-Scale Infrastructure for Chemistry and Aerosols (MUSICAv0). *Journal of Geophysical Research: Atmospheres*, *127*(16), e2022JD036650. https://doi.org/10.1029/2022JD036650

Tilmes, S., Hodzic, A., Emmons, L. K., Mills, M. J., Gettelman, A., Kinnison, D. E., et al. (2019). Climate forcing and trends of organic aerosols in the Community Earth System Model (CESM2). *Journal of Advances in Modeling Earth Systems*, *11*(12), 4323–4351. https://doi.org/10.1029/2019MS001827

Unger, N. (2014). On the role of plant volatiles in anthropogenic global climate change. *Geophysical Research Letters*, *41*(23), 8563–8569. https://doi.org/10.1002/2014GL061616

Val Martin, M., Logan, J. A., Kahn, R. A., Leung, F.-Y., Nelson, D. L., & Diner, D. J. (2010). Smoke injection heights from fires in North America: Analysis of 5 years of satellite observations. *Atmospheric Chemistry and Physics*, *10*(4), 1491–1510. https://doi.org/10.5194/acp-10-1491-2010

van der Werf, G. R., Randerson, J. T., Giglio, L., Collatz, G. J., Mu, M., Kasibhatla, P. S., et al. (2010). Global fire emissions and the contribution of deforestation, savanna, forest, agricultural, and peat fires (1997–2009). *Atmospheric Chemistry and Physics*, *10*(23), 11707–11735. https://doi.org/10.5194/acp-10-11707-2010

van der Werf, G. R., Randerson, J. T., Giglio, L., van Leeuwen, T. T., Chen, Y., Rogers, B. M., et al. (2017). Global fire emissions estimates during 1997–2016. *Earth System Science Data*, *9*(2), 697–720. https://doi.org/10.5194/essd-9-697-2017

Veira, A., Kloster, S., Schutgens, N. A. J., & Kaiser, J. W. (2015). Fire emission heights in the climate system—Part 2: Impact on transport, black carbon concentrations and radiation. *Atmospheric Chemistry and Physics*, *15*(13), 7173–7193. https://doi.org/10.5194/acp-15-7173-2015

Ward, D. S., & Mahowald, N. M. (2015). Local sources of global climate forcing from different categories of land use activities. *Earth System Dynamic*, *6*(1), 175–194. https://doi.org/10.5194/esd-6-175-2015

Ward, D. S., Mahowald, N. M., & Kloster, S. (2014). Potential climate forcing of land use and land cover change. *Atmospheric Chemistry and Physics*, *14*(23), 12701–12724. https://doi.org/10.5194/acp-14-12701-2014

Weber, J., King, J. A., Abraham, N. L., Grosvenor, D. P., Smith, C. J., Shin, Y. M., et al. (2024). Chemistry-albedo feedbacks offset up to a third of forestation's CO_2 removal benefits. *Science*, *383*(6685), 860–864. https://doi.org/10.1126/science.adg6196

WHO. (2021). *WHO global air quality guidelines*. World Health Organization.

Wiedinmyer, C., Kimura, Y., McDonald-Buller, E. C., Emmons, L. K., Buchholz, R. R., Tang, W., et al. (2023a). The Fire Inventory from NCAR version 2.5: An updated global fire emissions model for climate and chemistry applications. *Geoscientific Model Development*, *16*(13), 3873–3891. https://doi.org/10.5194/gmd-16-3873-2023

Wiedinmyer, C., Kimura, Y., McDonald-Buller, E. C., Emmons, L. K., Buchholz, R. R., Tang, W., et al. (2023b). Fire inventory from NCAR version 2 fire emission [Dataset]. *Computational and Information Systems Laboratory*. https://doi.org/10.5065/XNPA-AF09

Wu, S., Mickley, L. J., Kaplan, J. O., & Jacob, D. J. (2012). Impacts of changes in land use and land cover on atmospheric chemistry and air quality over the 21st century. *Atmospheric Chemistry and Physics*, *12*(3), 1597–1609. https://doi.org/10.5194/acp-12-1597-2012

Zhang, Q., Jimenez, J. L., Canagaratna, M. R., Allan, J. D., Coe, H., Ulbrich, I., et al. (2007). Ubiquity and dominance of oxygenated species in organic aerosols in anthropogenically-influenced Northern Hemisphere midlatitudes. *Geophysical Research Letters*, *34*(13). https://doi.org/10.1029/2007GL029979

References From the Supporting Information

Andela, N., & van der Werf, G. R. (2014). Recent trends in African fires driven by cropland expansion and El Niño to La Niña transition. *Nature Climate Change*, *4*(9), 791–795. https://doi.org/10.1038/NCLIMATE2313

Aragão, L. E. O. C., Malhi, Y., Barbier, N., Lima, A., Shimabukuro, Y., Anderson, L., & Saatchi, S. (2008). Interactions between rainfall, deforestation and fires during recent years in the Brazilian Amazonia. *Philosophical Transactions of the Royal Society B: Biological Sciences*, *363*(1498), 1779–1785. https://doi.org/10.1098/rstb.2007.0026

Butt, E. W., Conibear, L., Smith, C., Baker, J. C. A., Rigby, R., Knote, C., & Spracklen, D. V. (2022). Achieving Brazil's deforestation target will reduce fire and deliver air quality and public health benefits. *Earth's Future*, *10*(12), e2022EF003048. https://doi.org/10.1029/2022EF003048

Chen, Y., Hall, J., van Wees, D., Andela, N., Hantson, S., Giglio, L., et al. (2023). Multi-decadal trends and variability in burned area from the fifth version of the Global Fire Emissions Database (GFED5). *Earth System Science Data*, *15*(11), 5227–5259. https://doi.org/10.5194/essd-15-5227-2023

Fischer, E. V., Jacob, D. J., Yantosca, R. M., Sulprizio, M. P., Millet, D. B., Mao, J., et al. (2014). Atmospheric peroxyacetyl nitrate (PAN): A global budget and source attribution. *Atmospheric Chemistry and Physics*, *14*(5), 2679–2698. https://doi.org/10.5194/acp-14-2679-2014

Hantson, S., Kelley, D. I., Arneth, A., Harrison, S. P., Archibald, S., Bachelet, D., et al. (2020). Quantitative assessment of fire and vegetation properties in simulations with fire-enabled vegetation models from the Fire Model Intercomparison Project. *Geoscientific Model Development*, *13*(7), 3299–3318. https://doi.org/10.5194/gmd-13-3299-2020

Li, F., Bond-Lamberty, B., & Levis, S. (2014). Quantifying the role of fire in the Earth system – Part 2: Impact on the net carbon balance of global terrestrial ecosystems for the 20th century. *Biogeosciences*, *11*(5), 1345–1360. https://doi.org/10.5194/bg-11-1345-2014

Li, F., Val Martin, M., Andreae, M. O., Arneth, A., Hantson, S., Kaiser, J. W., et al. (2019). Historical (1700–2012) global multi-model estimates of the fire emissions from the Fire Modeling Intercomparison Project (FireMIP). *Atmospheric Chemistry and Physics*, *19*(19), 12545–12567. https://doi.org/10.5194/acp-19-12545-2019

Li, F., Song, X., Harrison, S. P., Marlon, J. R., Lin, Z., Leung, L. R., et al. (2024). Evaluation of global fire simulations in CMIP6 Earth system models. *Geoscientific Model Development*, *17*(23), 8751–8771. https://doi.org/10.5194/gmd-17-8751-2024

Tang, W., Tilmes, S., Lawrence, D. M., Li, F., He, C., Emmons, L. K., et al. (2023). Impact of solar geoengineering on wildfires in the 21st century in CESM2/WACCM6. *Atmospheric Chemistry and Physics*, *23*(9), 5467–5486. https://doi.org/10.5194/acp-23-5467-2023

Wan, H., Zhang, K., Vogl, C. J., Woodward, C. S., Easter, R. C., Rasch, P. J., et al. (2024). Numerical coupling of aerosol emissions, dry removal, and turbulent mixing in the E3SM Atmosphere Model version 1 (EAMv1) – Part 1: Dust budget analyses and the impacts of a revised coupling scheme. *Geoscientific Model Development*, *17*(3), 1387–1407. https://doi.org/10.5194/gmd-17-1387-2024